ISSN 2616-5767 Vol.7, Issue 5: 130-139, DOI: 10.25236/AJETS.2024.070517

Analysis of Lubrication Characteristics and Friction Coefficient of Steel/Plastic Spur Gear Pair under Grease Lubrication

Dechang Hu[1,a], Wei Cai[1,b], Jun Hu[1,c], Tongxing Zhou[2,d], Yangshou Xiong[3,e,*], Kang Huang[4,f]

[1]*China Yangtze River Power Co, Yichang, 443000, China*
[2]*Zhihuan Science and Technology Co., Ltd., Hefei, 230601, China*
[3]*Anhui Province Key Lab of Aerospace Structural Parts Forming Technology and Equipment, Hefei, 230009, China*
[4]*Anhui Key Laboratory of Digit Design and Manufacture, Hefei, 230009, China*
[a]*hu_dechang@ctg.com.cn,* [b]*cai_wei1@ctg.com.cn,* [c]*Hu_jun1@ctg.com.cn,*
[d]*tongxing.zhou@aiuitech.com,* [e]*xiongys@hfut.edu.cn,* [f]*hfhuang98@163.com*
[*]*Corresponding author*

Abstract: *Under the condition of grease lubrication, the elastohydrodynamic lubrication (EHL) of steel/plastic gear pair is simulated and analyzed to get the oil film thickness and pressure distribution at the contact point, as well as the influence of rotating speed and load on the friction coefficient. And the change of friction coefficient in the process of meshing is solved. The results are compared with those of steel/steel gear pair. The results show that the oil film of steel/plastic gear pair is thicker than that of steel/steel gear pair, but the pressure is less than that of steel/steel gear pair and there is no secondary pressure peak in the pressure distribution of steel/plastic gear pair. Besides, the friction coefficient increases with the increase of the load and speed, tend to 0 at the pitch point, increase from the meshing-in point to the pitch point, and decrease from the pitch point to the meshing-out point. Under the same load and speed, the friction coefficient of steel/plastic meshing is smaller than that of steel/steel meshing. These conclusions provide a certain theoretical reference for the tribodynamics analysis of steel/plastic gear pairs under grease lubrication conditions.*

Keywords: *Grease, Plastic gear, Elastohydrodynamic lubrication, Numerical simulation*

1. Introduction

Grease is one of the most commonly used lubricating materials. At present, most reducers are lubricated with grease. However, due to the non-linear relationship between the shear stress and shear strain rate of lubricating grease, which shows significant non-Newtonian fluid characteristics, the theoretical study of grease lubrication is much more difficult than that of oil lubrication [1].

In recent decades, domestic and foreign scholars have done some research on lubricating grease. Some scholars have measured the oil film thickness of lubricating grease by means of optical interferometry, magnetoresistance, capacitance through experiments, but they have not further studied the friction characteristics of lubricating grease [2-6]. Kanazawa Y et al. [7] studied the film formation characteristics and friction characteristics of contact points within a certain range of entrainment speed, surface roughness, and contact temperature through a ball-disk machine; Laurentis N D et al. [8] and David Gonçalves et al. [9] analyzed the relationship among the composition of bearing grease, film thickness and friction in lubricating contact. Singh J et al. [10] studied the friction and vibration characteristics of grease under the condition of point contact. All the above are experimental studies.

On the other hand, gear is the most widely used and most basic transmission method in mechanical transmission. We can see many pictures of plastic gears in the mechanical industry on the internet, such as the following two pictures. Existing research on plastic gears is mainly oriented to light and medium load conditions of 0-20Nm, and the application of plastic gears in engineering is also mainly concentrated in the geometric motion transmission such as auto parts as shown in Figure 1 which is provided by the industry users. In terms of transmitting greater power, there have been cases where plastic gears are applied to lifting equipment (300kg), and the weight of the whole machine is less than 20kg, which

ISSN 2616-5767 Vol.7, Issue 5: 130-139, DOI: 10.25236/AJETS.2024.070517

greatly reduces the weight of the product, as shown in Figure 2 which comes from electric hoist in our laboratory.

Figure 1: Plastic gear in auto parts

Figure 2: Plastic gear in lifting equipment

However, at present the research of metal / plastic gear, there are some drawbacks in more academics is the study of metal / plastic gear vibration problem. In these papers about metal/plastic gear lubrication more are in the condition of oil lubrication. So, choose metal / plastic gear research has great significance.

In this paper, a finite line contact EHL model of steel/plastic spur gear pair under grease lubrication is established, and the elastohydrodynamic lubrication analysis is carried out. The film thickness and pressure distribution of steel/plastic gear pair under the condition of grease lubrication and the change of friction coefficient in meshing are studied, which provides a theoretical reference for the tribodynamics analysis of steel/plastic gear pair. In this paper, the material is selected for PEEK plastic gear, this kind of material has high temperature resistance, comprehensive mechanical properties, wear resistance and strong chemical corrosion resistance, etc., is the top engineering plastics in molding gear nowadays.

2. Mathematical model

2.1. Calculation model and basic equation

2.1.1. Reynolds equation

The grease has a yield shear stress τ_s, and there is a non-shearing flow layer in the range of $\tau \leq \tau_s$. Only in the range of $\tau \leq \tau_s$, the grease will flow and show fluid properties [11]. As shown in Figure 3, h is the thickness of the oil film, h_p is the thickness of the non-shear layer, the z-axis is consistent with the thickness of the oil film, the y-axis is the leakage direction, and the x-axis is consistent with the direction of grease movement.

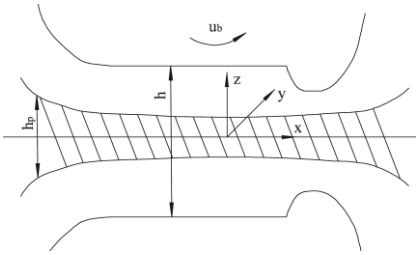

Figure 3: Flow of grease between relative surfaces

ISSN 2616-5767 Vol.7, Issue 5: 130-139, DOI: 10.25236/AJETS.2024.070517

There are three main constitutive equations to describe the rheological properties of lubricating grease currently:

Ostwald model:

$$\tau = \phi\dot{\gamma}^{n} \tag{1}$$

Bingham model:

$$\tau = \tau_s + \phi\dot{\gamma} \tag{2}$$

Herschel-Bulkley model:

$$\tau = \tau_s + \phi\dot{\gamma}^{n} \tag{3}$$

The constitutive equation of Herschel-Bulkley rheological model has strong adaptability and universality, and the calculated results are more accurate [12]. Therefore, Herschel-Bulkley model was adopted in this paper to establish an elastohydrodynamic model with finite long line contact grease.

The expression of Reynolds equation, a general form of grease lubrication based on constitutive equation of Herschel-Bulkley rheological model, is as follows:

$$\frac{\partial(\rho\mu_0 h)}{\partial x} + \frac{\partial(\rho v_0 h)}{\partial y} + \frac{\partial(\rho h)}{\partial t} = \frac{\partial(\rho G_R)}{\partial x} + \frac{\partial(\rho V_R)}{\partial y} \tag{4}$$

where, ρ is the lubricant density, μ_0 and v_0 are the velocity of the lubricant along the ox and oy directions:

$$\begin{cases} G_R = \left(\frac{1}{2}\right)^{\frac{(n+1)}{n}} \left(\frac{1}{\phi}\frac{\partial p}{\partial x}\right)^{\frac{1}{n}} (h - h_{px})^{\frac{(n+1)}{n}} \frac{n}{2n+1}(h + \frac{n}{n+1}h_{px}) \\ V_R = \left(\frac{1}{2}\right)^{\frac{(n+1)}{n}} \left(\frac{1}{\phi}\frac{\partial p}{\partial y}\right)^{\frac{1}{n}} (h - h_{py})^{\frac{(n+1)}{n}} \frac{n}{2n+1}(h + \frac{n}{n+1}h_{py}) \end{cases} \tag{5}$$

where h_{px} and h_{py} respectively represent the thickness of shear free flow layer in ox direction and oy direction.

As can be seen from the above formula, the Reynolds equation in its ordinary form is a two-dimensional second-order nonlinear partial differential equation, which is usually difficult to solve and requires a series of simplifications.

Under steady-state working condition, each physical quantity does not change with time, that is $\partial(\rho h)/\partial t = 0$, so Equation (4) can be simplified as

$$\frac{\partial(\rho\mu_0 h)}{\partial x} + \frac{\partial(\rho v_0 h)}{\partial y} = \frac{\partial(\rho G_R)}{\partial x} + \frac{\partial(\rho V_R)}{\partial y} \tag{6}$$

In the problem discussed in this paper, the motion direction of the lubricating surface follows x axis, while the velocity component of the lubricating surface along the direction of y axis is ignored. Therefore, $v_0 = 0$ and Equation (4) can be simplified as follows:

$$\frac{\partial(\rho\mu_0 h)}{\partial x} = \frac{\partial(\rho G_R)}{\partial x} + \frac{\partial(\rho V_R)}{\partial y} \tag{7}$$

For the linear contact problem, the leakage test is ignored. The oil film pressure p does not change along the direction of oy, that is $\partial p/\partial y = 0$, according to Equation (5), it can be obtained $V_R = 0$. Therefore, based on the constitutive equation of Herschel-Bulkley rheological model, the Reynolds equation of steady state grease line contact elastohydrodynamic lubrication can be expressed as:

$$\frac{\partial(\rho\mu_0 h)}{\partial x} = \frac{\partial(\rho G_R)}{\partial x} \tag{8}$$

Substituting y into Equation (8) and integrate x to obtain:

$$\rho\mu_0 h = \rho\left(\frac{1}{2}\right)^{\frac{(n+1)}{n}} \left(\frac{1}{\phi}\frac{dp}{dx}\right)^{\frac{1}{n}} (h - h_{px})^{\frac{(n+1)}{n}} \frac{n}{2n+1}(h + \frac{n}{n+1}h_{px}) + C \tag{9}$$

ISSN 2616-5767 Vol.7, Issue 5: 130-139, DOI: 10.25236/AJETS.2024.070517

C is a constant in Equation (9). After changing Equation (9), the Reynolds equation for contact elastohydrodynamic lubrication of steady-state grease line based on the constitutive equation of Herschel-Bulkley rheological model can be obtained as follows:

$$\frac{dp}{dx}=\frac{2\phi\rho^{-n}(\rho\mu_0 h-C)^n[2(2+\frac{1}{n})]^n}{(h-h_{px})^{n+1}(h+\frac{n}{n+1}h_{px})^n} \tag{10}$$

From Equation (1) and Equation (3), it can be seen that the yield shear stress $\tau_s=0$ is set on the basis of the grease Lubrication Reynolds equation of Herschel-Bulkley Model, thus obtaining the grease lubrication Reynolds equation of Ostwald model, that is, the thickness of the shear-free flow layer $h_{px}=0$. So, the Reynolds equation based on the constitutive equation of Ostwald model as follow [13]:

$$\frac{dp}{dx}=\frac{2\phi\rho^{-n}(\rho\mu_0 h-c)^n[2(2+\frac{1}{n})]^n}{h^{2n+1}} \tag{11}$$

2.1.2. Governing equation

In the analysis of elastohydrodynamic lubrication of metal gear pairs, only the elastic deformation of the contact surface of the gear is often considered; while the steel/plastic gear pair has a large plastic deformation when contacted. In this paper, plastic deformation and elastic deformation are combined to obtain the elastoplastic deformation of the contact surface.

As shown in Figure 4, the thickness of the elastohydrodynamic oil film is composed of two parts: the clearance $h_c+x^2/2R$ between the two surfaces when there is no elastic deformation, and the elastic-plastic deformation $v(x)$ on the contact surface caused by the compression of EHF film.

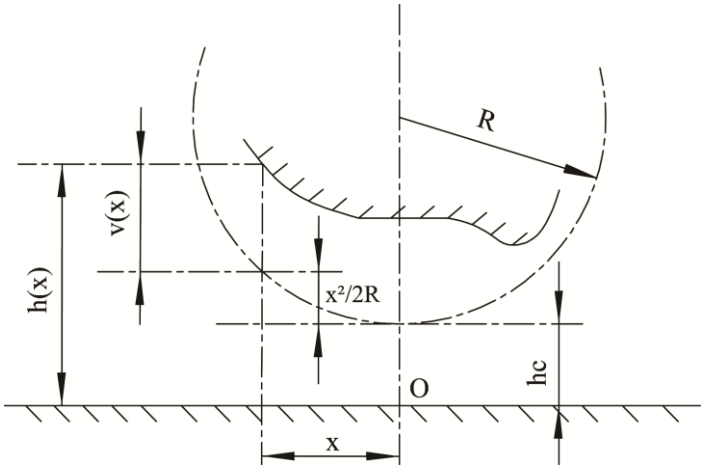

Figure 4: Oil film thickness diagram

The numerical calculation formula for the thickness of the line contact EHL film is expressed by the following:

$$\begin{cases} h(x)=h_c+\dfrac{x^2}{2R}+v(x) \\ v(x)=-\dfrac{2}{\pi E'}\displaystyle\int_{S_2}^{S_1}p(s)ln(s-x)^2ds+C' \end{cases} \tag{12}$$

In Equation (12), h_c is the distance between the contact surfaces without elastic deformation, R is the equivalent radius and $1/R=1/R_1+1/R_2$, where R_1 and R_2 are the curvature radius of the two contact surfaces respectively, s is additional coordinate of the x axis, $p(s)$ is the load distribution function. In practice, when the steel/plastic gear pair is meshed, the plastic gear will have a certain plastic deformation C'. Therefore, this article intends to combine the plastic deformation C' with h_c, and determine it when balancing the load; E' Is the equivalent elastic modulus,

$$\frac{1}{E'}=\frac{1}{2}(\frac{1-\mu_1{}^2}{E_1}+\frac{1-\mu_2{}^2}{E_2}) \tag{13}$$

ISSN 2616-5767 Vol.7, Issue 5: 130-139, DOI: 10.25236/AJETS.2024.070517

In this formula, μ_1 and μ_2 are the Poisson's ratios of the two contact surface materials, E_1 and E_2 are the elastic modulus of the two contact surface materials, respectively.

For isothermal conditions, the viscosity pressure equation is

$$\phi = \phi_0 exp\{(ln\phi_0 + 9.67)[(1 + p/p_0)^z - 1]\} \tag{14}$$

where ϕ_0 is the ambient viscosity of the grease, that is, the lubricant viscosity when $p = 0$ and $T = T_0$, and the initial temperature of T_0 is generally set at 303K. p_0 is the pressure-viscosity coefficient, and $p_0 = 1.96 \times 10^8$.

Density-pressure equation:

$$\rho = \rho_0(1 + \frac{C_1 p}{C_2}) \tag{15}$$

where $C_1 = 0.6 \times 10^{-9} Pa^{-1}$, $C_2 = 1.7 \times 10^{-9} Pa^{-1}$, ρ_0 is the environmental density of the grease.

The load balance equation is

$$\omega = \int_{x_{in}}^{x_{out}} p dx \tag{16}$$

where x_{in} and x_{out} are the entrance and exit coordinates of the calculation domain respectively, ω is the load per unit length.

The boundary conditions are $p(x_{in}) = 0; p(x_{out}) = \frac{\partial p}{\partial x} = 0,\ p \geq 0 (x_{in} < x < x_{out})$

The friction between the two surfaces is

$$F = -(F_1 + F_2)/2 \tag{17}$$

Where

$$\begin{cases} F_1 = \int_{x_{in}}^{x_{out}} \tau|_{z=0} dx \\ F_2 = \int_{x_{in}}^{x_{out}} \tau|_{z=h} dx \end{cases} \tag{18}$$

where F_1 and F_2 are the frictional forces on the upper and lower surfaces respectively, and both are forces per unit length, F is the average value of friction per unit area.

The friction coefficient is

$$\mu = \frac{F}{\omega} \tag{19}$$

2.1.3. A simplified model for gear meshing

The gear meshing model can be simplified as the relative contact between a plane and a cylinder with equivalent radius R, as shown in Figure 5.

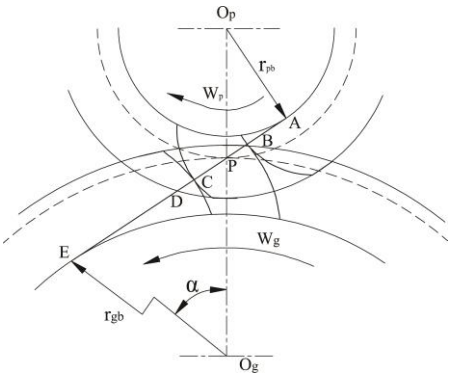

(a) Contact pattern of spur gear

ISSN 2616-5767 Vol.7, Issue 5: 130-139, DOI: 10.25236/AJETS.2024.070517

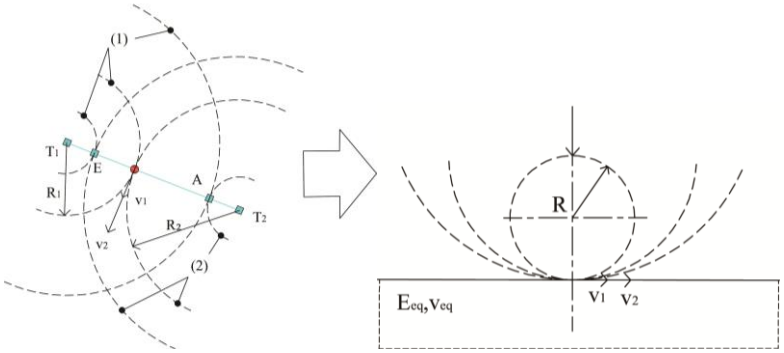

(b) A Simplified model of gear meshing

Figure 5: Diagram of gear meshing

The pitch radii of the two gears are

$$\begin{cases} r_1 = \dfrac{a}{i+1} \\ r_2 = \dfrac{ai}{i+1} \end{cases} \tag{20}$$

where, a is the center distance of two gears and i is the transmission ratio.

The radius of curvature at the meshing points of the gear teeth are as follows:

$$\begin{cases} R_1 = r_1 sin\alpha + s \\ R_2 = r_2 sin\alpha - s \end{cases} \tag{21}$$

where, α is the pressure angle of the gear, s is the distance from the meshing point to the pitch point.

Then the equivalent curvature radius is

$$\mathrm{R} = \frac{R_1 R_2}{R_1 + R_2} = \frac{(r_1 sin\alpha + s)(r_2 sin\alpha - s)}{(r_1 + r_2) sin\alpha} \tag{22}$$

The lubricating entrainment velocity is

$$\mathrm{v} = \frac{v_1 + v_2}{2} \tag{23}$$

where v_1 and v_2 are the tangential velocity of driving gear and driven gear, and their expressions are as follows:

$$\begin{cases} v_1 = \dfrac{\pi n_1}{30}(r_1 sin\alpha + s) \\ v_2 = \dfrac{\pi n_2}{30}(r_2 sin\alpha - s) \end{cases} \tag{24}$$

where n_1 and n_2 are the rotational speeds of the driving and driven gears respectively.

2.2. Dimensionless equation

The dimensionless parameters in this paper are as follows: film thickness $\bar{h} = hR/b^2$, load $\bar{\omega} = \omega/E'R$, speed in the x direction $\bar{\mu} = \phi_0\mu/E'R$, Distance in x direction $\bar{x} = x/b$, oil film pressure $\bar{p} = p/p_H$, viscosity $\bar{\phi} = \phi/\phi_0$, density $\bar{\rho} = \rho/\rho_0$. Among them, p_H is the maximum Hertz contact stress, $p_H = 2\omega/(\pi b)$; b is the half width of the Hertz contact region, and $b = (8\omega R/\pi E')^{0.5}$.

The dimensionless equation is as follows:

1) Dimensionless Reynolds equation:

$$\frac{d}{d\bar{x}}\left[\varepsilon\left(\frac{d\bar{p}}{d\bar{x}}\right)^{\frac{1}{n}}\right] = \frac{d(\bar{\rho}\bar{h})}{d\bar{x}} \tag{25}$$

ISSN 2616-5767 Vol.7, Issue 5: 130-139, DOI: 10.25236/AJETS.2024.070517

where $\varepsilon = \frac{1}{K}\frac{\bar{p}}{\bar{\phi}^{1/n}}\bar{h}^{(2+1/n)}$, $K = \frac{2n}{2n+1}\frac{R}{\mu b^2}\left(\frac{p_H}{\phi_0 b}\right)^{1/n}\frac{b^{2(2+1/n)}}{2R}$. The boundary condition of entrance area is $\bar{p}(\bar{x}_{in}) = 0$, the boundary conditions of exit area are $\bar{p}(\bar{x}_{out}) = 0$ and $\frac{d\bar{p}(\bar{x}_{out})}{d\bar{x}} = 0$.

2) Dimensionless film thickness equation:

$$\overline{h(x)} = \overline{h_0} + \frac{\bar{x}^2}{2} - \frac{1}{\pi}\int_{\bar{x}_{in}}^{x_{out}} \bar{p}(s)\cdot ln|\bar{x}-s|ds + C' \tag{26}$$

In this formula, $\overline{h_0}$ is a dimensionless constant, which can be obtained during the solution process.

3) Dimensionless viscosity-pressure equation:

$$\bar{\phi} = exp\{(ln\phi_0 + 9.67)[(1+5.1\times10^{-9}p)^z - 1]\} \tag{27}$$

4) Dimensionless density-pressure equation:

$$\bar{\rho} = (1 + \frac{C_1\bar{p}}{1+C_2\bar{p}}) \tag{28}$$

where $C_1 = 0.6\times10^{-9}p_H$, $C_2 = 1.7\times10^{-9}p_H$.

5) Dimensionless load balance equation:

$$\int_{\bar{x}_{in}}^{\bar{x}_{out}} \bar{p}d\bar{x} = \frac{\pi}{2} \tag{29}$$

3. Numerical solution

3.1. Discretization of equations

Discretize Equation (29) by the finite difference method, and the discretized difference equation of the Reynolds equation is

$$\frac{\varepsilon_{i+1/2}\overline{(p_{i+1}} - \bar{p}_i)^{1/n} - \varepsilon_{i-1/2}\overline{(p_i} - \bar{p}_{i-1})^{1/n}}{\Lambda\bar{x}^{1+1/n}} = \frac{\bar{p}_i\bar{h}_i - \bar{\rho}_{i-1}\bar{h}_{i-1}}{\Lambda\bar{x}} \tag{30}$$

where $\varepsilon_{i\pm1/2} = \frac{1}{2}(\varepsilon_i + \varepsilon_{i\pm1})$, $\Delta\bar{x} = \Delta\bar{x}_i - \Delta\bar{x}_{i-1}$.

The discrete form of the film thickness equation is

$$\bar{h}(\bar{x}_i) = \bar{h}_0 + \frac{\bar{x}_i^2}{2} - \frac{1}{\pi}\sum_{i=1}^{n} k_{i,j}\bar{p}_j(\bar{x}_j) \tag{31}$$

where $k_{i,j}$ is the coefficient of elastic deformation.

The discrete load balance equation is

$$\Delta\bar{x}\sum_{i=0}^{n-1}\frac{(\bar{p}_i + \bar{p}_{i+1})}{2} = \frac{\pi}{2} \tag{32}$$

3.2. Numerical solution method

Use the multi-grid method to solve the pressure, and the elastic deformation is solved by the multi-grid integration method. The number of grid layers in this paper is 4 and the top-level grid node is 129. Use the finite difference method to solve the Reynolds equation. The initial pressure adopts Hertz pressure distribution. The iterative convergence criterion for solving Reynolds equation is the criterion of relative accuracy, which is $\varepsilon_1 = \varepsilon_2 = 1\times10^{-3}$.

ISSN 2616-5767 Vol.7, Issue 5: 130-139, DOI: 10.25236/AJETS.2024.070517

4. Discussion of results

In this paper, the material of the plastic large gear is PEEK, the number of gear teeth $z_2 = 147$, the elastic modulus $E_2 = 1.31 \times 10^{10} Pa$, Poisson's ratio $\mu_2 = 0.42$, and the number of steel pinion teeth $z_1 = 47$, the elastic modulus $E_1 = 2.06 \times 10^{11} Pa$, Poisson's ratio $\mu_1 = 0.3$; Modulus $m = 2.5mm$; Width $B = 20mm$. It can be calculated that the equivalent elastic modulus of plastic / steel is $E' = 2.97 \times 10^{10} Pa$. The simplified gear load spectrum is shown in Figure 6.

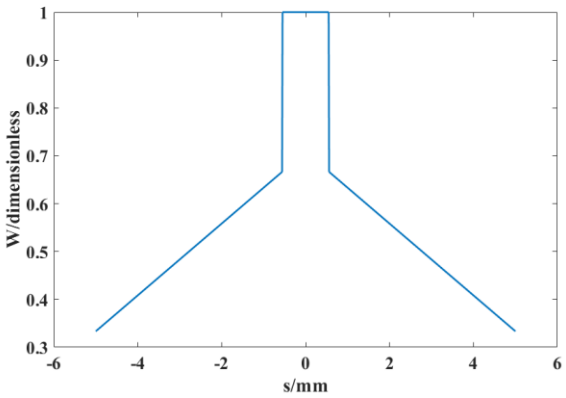

Figure 6: Variation of load with distance from meshing point to pitch point

4.1. Film thickness and pressure distribution

When $W = 2000N$, $n = 960r/min$, the film thickness and pressure distribution at the pitch points are shown in the figure below:

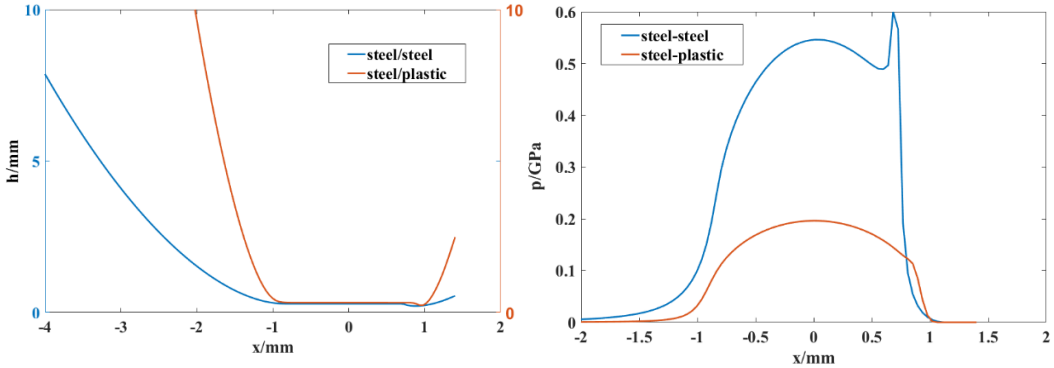

(a)Film thickness distribution *(b)Pressure distribution*

Figure 7: Film thickness and pressure distribution of steel/plastic and steel/steel gear pairs at pitch point at $W = 2000N$, $n = 960r/min$

It can be seen from Fig. 7 that there is no pressure spike in the EHL film pressure distribution of the steel/plastic gear pair, and the maximum oil film pressure is mainly in the center of the contact area, and under the same load and speed, the oil film pressure of the steel/plastic gear pair is less than that of the steel/steel gear pair. There is no obvious necking phenomenon in oil film thickness distribution and the film thickness of steel/plastic gear pair is larger than that of steel/steel gear pair. In reference, the author studied the film thickness and pressure comparison of steel/plastic gear pair and steel/steel gear pair under oil-lubricated conditions, and the same results were obtained. It can be seen that the film thickness of steel/plastic gear pair will be thicker and the pressure will be lower in either real oil lubrication or grease lubrication, and there will be no secondary peak. And figure 9 found through observation, on-Newtonian fluid lubrication oil pressure size may be associated with oil film thickness, oil pressure and decreased along with the oil film thickness.

4.2. Effect of load on friction coefficient

Figure. 8 shows the change curve of friction coefficient of steel/steel and steel/plastic gear pair under different loads when $n = 960r/min$. It can be seen from the figure that, with the increase of load, the

ISSN 2616-5767 Vol.7, Issue 5: 130-139, DOI: 10.25236/AJETS.2024.070517

friction coefficient of steel/steel gear pair and steel/plastic gear pair increases; Similarly, it can be seen from Figure. 5 that the friction coefficient of steel/plastic meshing is smaller than that of steel/steel meshing. Under the same load and rotating speed, the oil film pressure of steel/plastic meshing is less than that of steel/steel meshing. According to the relationship between viscosity and pressure, the viscosity of lubricating grease decreases, then the shear force decreases greatly, so the friction coefficient of steel/plastic gear pair is smaller than that of steel/steel gear pair. Different from steel/steel gear pair, the change of friction coefficient of steel/plastic gear pair does not fluctuate from meshing-in point to meshing-out point. Because there is secondary pressure peak in the oil film distribution of steel/steel gear pair and for different meshing points, the position of the secondary pressure peak changes, but there is no secondary pressure peak in steel/plastic gear pair, so the change of friction coefficient is more regular.

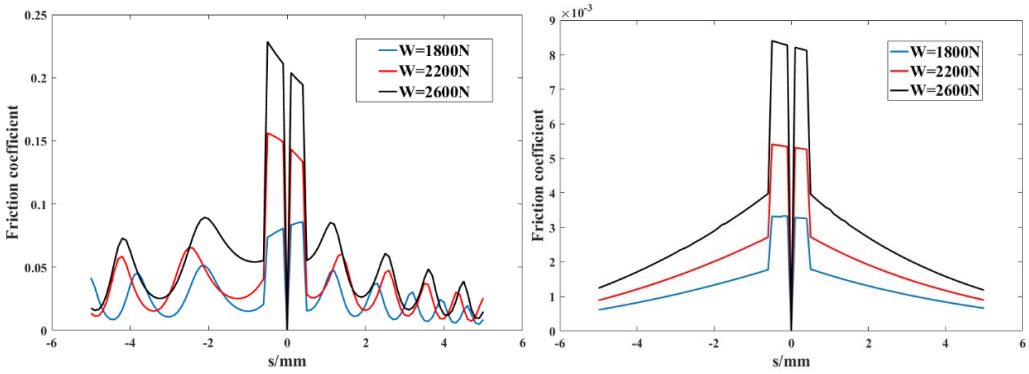

(a)steel/steel *(b)steel/plastic*

Figure 8: Friction coefficient of steel/steel and steel/plastic gear pair at $n = 960r/min$, for different loads

4.3. Effect of rotating speed on friction coefficient

Figure 9 is the friction coefficient change curve of steel/steel and steel/plastic gear pair at different rotational speeds when $W = 2000N$. It can be seen from the figure that the friction coefficient increases with the increase of load; And the friction coefficient at the pitch point tends to 0, owing to the pure rolling. Besides, in the meshing area of single pair of teeth, the friction coefficient is larger due to the larger load. As a result, the change trend of friction coefficient is gradually increasing from the meshing-in point to the pitch point, and gradually decreasing from the pitch point to the meshing-out point. Like the reason in Figure 8, the friction factor of the steel-steel gear pair in Figure 9 also fluctuates from the tapping point to the tapping point.

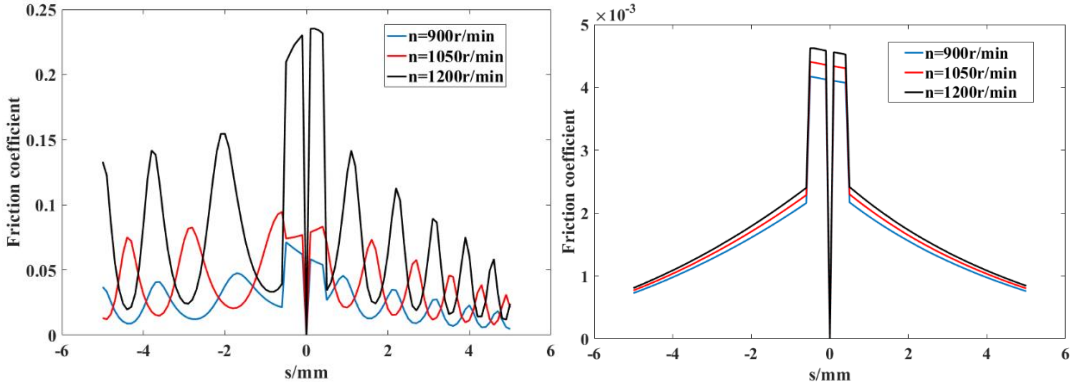

(a)steel/steel *(b)steel/plastic*

Figure 9: Friction coefficient of steel/steel and steel/plastic gear pair at $W = 2000N$, for different rotation speeds

5. Conclusion

In this paper, a finite line contact EHL model of steel/plastic spur gears under grease lubrication conditions is proposed, and numerical simulation analysis is performed to solve the film thickness pressure distribution and friction coefficient, which provides a certain theoretical reference for the

ISSN 2616-5767 Vol.7, Issue 5: 130-139, DOI: 10.25236/AJETS.2024.070517

tribodynamics analysis of steel/plastic gear pairs under grease lubrication conditions. The results show that:

(1) Due to the large elastic-plastic deformation of the steel/plastic meshing, there is no obvious necking phenomenon in the oil film thickness distribution of the steel/plastic gear pair, and the oil film thickness is greater than that of the steel/plastic gear pair. The pressure distribution of the steel/plastic gear pair did not show a secondary pressure peak, and the pressure was significantly smaller than that of the steel/steel gear pair. The pressure distribution of the steel/plastic gear pair did not show a pressure spike, and the pressure was significantly smaller than that of the steel/steel gear pair.

(2) The friction coefficients of the steel/plastic and the steel/steel gear pair increase with the increasement of the speed and load, tend to 0 at the pitch point, increase from the meshing-in point to the pitch point, and decrease from the pitch point to the meshing-out point. Besides, under the same load and speed, the friction coefficient of steel/plastic meshing is smaller than that of steel/steel meshing.

Acknowledgements

This work is supported by Natural Science Foundation of Anhui Province (1908085QE228).

References

[1] Jiang M J and Guo X C. Performance and application of grease, China Petroleum Press, Beijing.2010
[2] Wedeven L D, Evans D, Cameron A. Optical analysis of ball bearing starvation. J. Lubr. Technol 1971, 93(3):349-361.
[3] Poon S Y.An Experimental Study of Grease in Elastohydrodynamic Lubrication. J. Lubr. Technol 1972, 94(1):27.
[4] Aihar S, Dowson D.A study of film thickness in grease lubricated elastohydrodynamic contacts. In: Proceedings of 5th Leeds—Lyon Symposium on Tribology, London. Mechanical Engineering Publishers, pp.1978, 104-115.
[5] Cen H, Lugt P M, Morales-Espejel G. On the Film Thickness of Grease-Lubricated Contacts at Low Speeds. Tribo. Trans 2014, 57(4):668-678.
[6] David Gon ̧alves, Beatriz Gra ̧a, Campos A V et al. On the film thickness behaviour of polymer greases at low and high speeds. Tribo. Int 2015, 90: 435-444.
[7] Kanazawa Y, Sayles R S, Kadiric A. Film formation and friction in grease lubricated rolling-sliding non-conformal contacts. Tribo. Int 2017, 109: 505-518.
[8] Laurentis N D, Kadiric A, Lugt P et al. The Influence of Bearing Grease Composition on Friction in Rolling/Sliding Concentrated Contacts. Tribo. Int 2017, 94: 624-632.
[9] David Gon ̧alves, Beatriz Gra ̧a, Campos A V et al. On the friction behaviour of polymer greases. Tribo. Int 2016, 93:399-410.
[10] Singh J, Kumar D, Tandon N. Tribo-Dynamics of Nanocomposite Grease Lubricated Point Contact Under Elastohydrodynamic Lubrication Regime. J. Tribol 2019, 141(3): 031501.
[11] Li G. Film forming Mechanism and Lubrication Characteristics of Grease under harsh conditions [D]. Tsinghua University.2010
[12] Bair S, Winer W O. Shear strength measurements of lubricants at high pressure[J]. ASME Journal of Lubrication Technology 1979, 10l: 251-257.
[13] Wang Y S, Yang B Y, Su B, et al. Application of elastoplastic flow model in elastohydrodynamic lubrication characteristics analysis [J]. Journal of tribology 2005, 25(2):159-163.